Perturbation from a Distance: Mutations that Alter LacI Function through Long-Range Effects†

Liskin Swint-Kruse,‡,§ Hongli Zhan,§ Bonnie M. Fairbanks,§,|| Atul Maheshwari,§,⊥ and Kathleen S. Matthews*,‡,§

W. M. Keck Center for Computational Biology and Department of Biochemistry and Cell Biology, M.S. 140, Rice University, 6100 South Main Street, Houston, Texas 77005

Received June 27, 2003; Revised Manuscript Received October 8, 2003

ABSTRACT: Allosteric modification of ligand binding is central to LacI transcription control. Recently, the conformational change between LacI operator- and inducer-bound states was simulated with targeted molecular dynamics (TMD) [Flynn, T. C., Swint-Kruse, L., Kong, Y., Booth, C., Matthews, K. S., and Ma, J. (2003) *Protein Sci., 12,* 2523−2541]. Atomic-level analyses of TMD results indicate the structural importance of the core pivot region that connects the N- and C-subdomains flanking the inducer-binding site. Further, a number of LacI mutations in the core pivot have been identified recently by their altered behaviors in phenotypic screens. Biochemical characterization of three of these variants—L148F, S151P, and P320A—provides an opportunity to directly explore the role of the core pivot in repressor function. For L148F, inducer IPTG binding affinity is strengthened, whereas O^1 operator DNA binding is diminished ∼30-fold. In contrast, O^1 binding is increased for S151P, whereas IPTG binding is decreased. UV-difference spectroscopy and urea denaturation indicate long-range effects in both variants. Interestingly, P320A binds to DNA ∼4-fold more tightly than wild-type, yet inducer binding is unaffected. To examine linkage between the core pivot and DNA binding domains, the L148F substitution was combined with Q60G, a previously known mutant with enhanced operator affinity. The double mutant exhibits the properties of both parent proteins, resulting in near wild-type DNA binding affinity and enhanced inducer sensitivity. These features may render Q60G/L148F more cost-effective in technological applications than wild-type repressor. As a group, the behaviors of the core pivot mutants are consistent with the allosteric structural role predicted for this region by TMD and reflect the significant long-range impact that single substitutions can elicit on protein function.

The core domains of the LacI/GalR repressor proteins, the periplasmic binding proteins (PBPs),[1] and the extracellular domains of many G-protein coupled receptors (GPCRs) have a common fold, which comprises two interconnected subdomains flanking a small-molecule binding site (*2*−*14*). Generally, ligand-binding to these proteins results in structural changes that are utilized to transmit signals. In the LacI/GalR family, these structural alterations result in genetic regulation (e.g., ref *15*). For the PBPs, structural shifts provide information on availability/transport of small molecules in the environment (*4*, *5*). For the GPCR family, structural changes in the extracellular domain in response to ligand binding effect a variety of intracellular alterations (e.g., refs *11*, *14*, and *16*−*18*). Given the functional importance of the fold common to these disparate proteins, the significant information available on the lactose repressor protein (LacI) provides an opportunity to ascertain the mechanism by which binding information is transmitted to distant regions of a protein.[2]

Structure determination is an indispensable tool for understanding conformational change. For LacI, crystal structures are available for the large, dimeric core domains (∼280 amino acids/monomer; Figure 1A,B), (*6*, *7*, *19*, *20*) in several liganded states. These models provide information about the binding sites as well as the structural differences of the functionally distinct conformations. However, their static nature precludes understanding the dynamics critical to function. With the recent availability of enhanced computing power, these "fixed" models may be coupled with

† This work was supported by NIH Grant GM22441 and Robert A. Welch Grant C-576 to K.S.M. L.S.K. was supported in part by a fellowship from the Keck Center for Computational Biology (National Library of Medicine Grant LM07093).

* To whom correspondence should be addressed. Telephone (713) 348−4871. Fax (713) 348−6149. Email: ksm@rice.edu.

‡ W. M. Keck Center for Computational Biology.

§ Department of Biochemistry and Cell Biology.

|| Current address: Department of Biological Sciences, Auburn University, Auburn, Alabama 36849.

⊥ Current address: Baylor College of Medicine, Houston, Texas 77030.

[1] Abbreviations: GPCR, G-protein coupled receptor; IPTG, isopropyl-*β*,D-thiogalactoside; LacI, lactose repressor protein; MUG, 4-methylumbelliferyl-*β*,D-galactoside; ONPF, *o*-nitrophenyl-*β*,D-fucoside; PCR, polymerase chain reaction; PBP, periplasmic binding proteins; TMD, targeted molecular dynamics simulations; Xgal, 5-bromo-4-chloro-3-indolyl-*β*,D-galactoside.

[2] The *lac* repressor protein (LacI) exerts its repression function via binding to its target operator DNA sequence with high affinity, thereby inhibiting RNA polymerase transcription of the downstream lactose metabolic genes. DNA binding occurs via an N-terminal DNA-binding domain. A separate ligand-binding site on the LacI core domain recognizes a small-molecule inducer sugar. Binding to inducer results in a protein conformational change through which the sequence-specific DNA-binding affinity of LacI is reduced by $>10^4$. LacI thus vacates operator DNA, and repression is relieved (for review, see ref *1*).

10.1021/bi035116x CCC: $25.00
Published on Web 11/06/2003

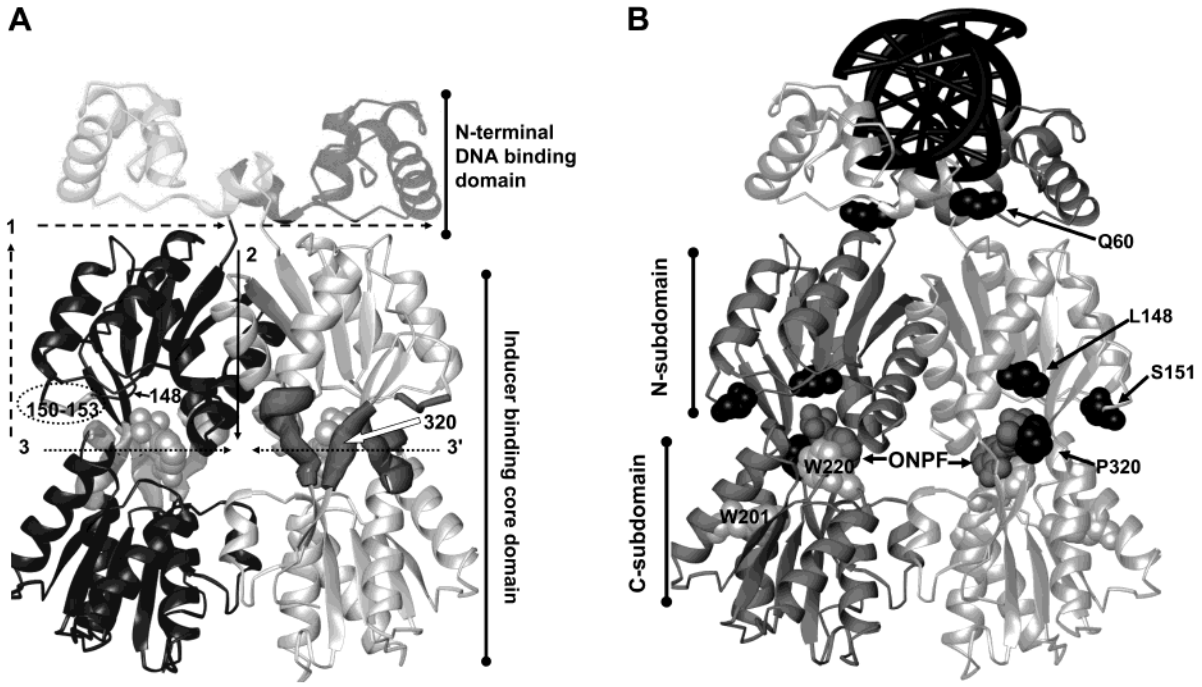

FIGURE 1: (A) Core pivot region and allosteric pathway for LacI response to inducer from targeted molecular dynamics simulations (*23*). The dimeric structure shown is from Protein Data Bank file 1efa (*6*). One monomer is dark gray, and the other is light gray. The protein consists of an N-terminal DNA binding domain, the N- and C-subdomains (see Figure 1B) of the core flanking the inducer binding site, and the C-terminal oligomerization motif that facilitates tetramer formation (not present in the dimer structure shown). The three strands and two loops comprising the core pivot are indicated on the structure with a wider ribbon in contrasting colors. Anti-inducer ONPF is represented with a light gray spacefilling model. The shaded area covering the DNA binding domain indicates that this region was not included in the simulation, since this region is not resolved in the IPTG-bound structure and identical atoms must be included in the simulation. The dotted circle denotes the flexible loop that includes S151P and is near to D149, which appears to instigate the conformational change. Positions for L148 and P320 are also indicated. Arrows labeled 1, 2, and 3 depict the direction of the allosteric pathway, which begins within a single "trigger" monomer (dark gray). Pathway 1 (long dash) initiates at D149 and is transmitted along the outside of the protein to the N-subdomain·N-terminal interface and then travels down the N-subdomain subunit interface (pathway 2; solid arrow), affecting both monomers. Changes similar to pathway 1 then occur at the top of the "response" monomer N-subdomain (light gray), indicated by the continuation of the dashed line on the darker monomer. Over the time frame of pathways 1 and 2, structural changes also occur across the bottom of the inducer-binding site between the N- and C-subdomains (pathway 3; dotted arrow). The backbones of the β-strands in the core pivot near P320 show significant changes in ϕ and ψ values during the simulation. Removing the proline at position 320 therefore has the potential to increase the flexibility in this region. This overall path for allosteric change is consonant with the broad spectrum of data for LacI available from genetic, biochemical, and biophysical studies. (B) Structure of LacI with positions of relevant mutations. The structure of the dimeric form of LacI bound to DNA (top, black ladder) and anti-inducer, ONPF (gray spacefilling), is shown. ONPF occupies the inducer-binding site. The dimer is the DNA binding unit. One monomer is colored dark gray, the other monomer light gray. The coordinates are from Protein Data Bank File 1efa (*6*). The side chains mutated in the variant proteins and presented in this study are shown in black spacefill (Q60, L148, S151, P320). The side chains of W201 and W220, which are responsible for intrinsic fluorescence, are shown by light gray spacefilling models. Note that Q60 is located at the end of the hinge helix that connects the DNA binding and core domains, in the cross-domain interface critical to allosteric communication (*6, 74*).

computer simulations that use equations of motion to predict structural fluctuations and/or changes. Targeted molecular dynamics (TMD) provide an especially promising avenue for simulating the molecular pathway between two known, end-point conformations (*21*, *22*). Such calculations may be accomplished more quickly and for larger systems than unrestrained simulations. Recently, we have utilized TMD simulations using the DNA- and inducer-bound conformations of the core domain of LacI (Figure 1A) (*23*). Detailed analyses of the results indicate that a number of residues in the "core pivot" region, which connects the N- and C-subdomains that flank the inducer-binding site, are important to the allosteric conformational change.

Mutations in this core pivot region have been identified recently from two different phenotypic screens: The first searched for second-site mutations that restored repression to the monomeric Y282D protein (*24*), and the second identified LacI variants with altered inducer properties (described herein). At the time the screens were executed, mutations in the core pivot were not anticipated to evince their respective phenotypes, leading to the conclusion that these variants must have long-range conformational effects (*24*). This hypothesis was supported by the recent TMD results (*23*). Biochemical characterization of three representative LacI variants from the screens (L148F, S151P, and P320A; Figure 1B) provides the opportunity to examine the putative long-range conformational effects that must underlie the observed phenotypic behavior. We have pursued a range of experiments to illuminate these properties: spectroscopic analysis, measurement of binding affinities, operator release, and chemical denaturation. The data accumulated indicate significant functional and structural changes compared to wild-type LacI.

In addition, we used one of these variants to explore the structural linkage between the core pivot region and the interface between the core N-subdomain and the DNA-binding domain. L148F, which exhibits diminished operator binding and enhanced inducer binding, was combined with

the previously known Q60G mutation (Figure 1B), which has enhanced operator affinity and wild-type inducer binding (*25*). The double mutant retains features of both parent proteins: Repression is enhanced compared to the L148F single mutation, but induction still occurs at lower IPTG concentrations. Lastly, since LacI has been exploited for many commercial purposes that require inducible control of recombinant protein expression, Q60G/L148F potentially can alleviate the considerable cost of IPTG used for induction.

MATERIALS AND METHODS

Plasmids and Mutagenesis. Restriction endonucleases, thermostable DNA polymerase, dNTPs, and related reagents were purchased from either Promega (Madison, WI) or New England Biolabs, Inc. (Beverly, MA).

To facilitate phenotypic screening of the induction function, a new plasmid containing the LacI gene was constructed by excising *lacI* and related promoters from the plasmid pLS1 (*24*) with EcoRI and inserting this fragment into the EcoRI site of pBR322. The resulting plasmid, named pCRE, has the low plasmid copy number and ampicillin resistance of pBR322 but expresses the *lacI* gene under control of the strong I^q promoter of pLS1.

For random mutagenesis, the *lacI* gene of pLS1 or pCRE was subjected to error-prone PCR amplification based upon the protocol of Fromant et al. (*26*). This procedure encourages base substitution via increased concentration of $MgCl_2$ (>4 mM final concentration), addition of $MnCl_2$ (0.5 mM), as well as including a large excess of one of the four dNTPs (>3 mM, compared to 0.25 mM of the remaining three dNTP species, leading to four different amplification reactions). Amplification utilized the following primers: (i) 5′-GCCCGTGCATATGAAACCAGTAACGTTATACGATGTC-3′ and (ii) 5′-CCCCGAATTCTCATTACTGCCCGCTTTCCAGTCG-3′ (Genosys Inc., Houston, TX). The PCR product was treated with *Sac*I and *Kas*I to generate strand scission at internal sites, small fragments were removed with the QIAquick PCR Purification Kit (Qiagen), and the resulting insert was ligated into the vector, pCRE, from which the corresponding wild-type sequence was removed. In the *lacI* gene, the *Sac*I site occurs in the codon for amino acid 45, while the *Kas*I site is concurrent with the codon for amino acid 328. Thus, random mutagenesis was limited to the LacI core domain and did not affect either the DNA binding region or tetramerization domain. The resulting, randomly mutated pCRE was amplified from the ligation mixture by transforming the ligation reaction into "MAX efficiency" DH5α cells (Gibco BRL/Invitrogen Corp.; Carlsberg, CA), growing all transformants in 5 mL of LB media, and purifying mixed plasmid with a QIAprep Spin Miniprep Kit (Qiagen). Mutated pCRE was transformed into *Escherichia coli* 3.300 cells (Hfr/*lacI*22 *relA1 spo*T1 *thi*-1; E. coli Genetic Stock Center, Yale University) (*27*). Single plasmids were purified from a number of colonies, and their *lacI* genes were sequenced; random mutagenesis resulted between 0 and 22 mutations per *lacI* gene (1080 basepairs).

The gene encoding the S151P/Y282D double mutant was identified on the plasmid pAC1 (*28*, *29*). The Y282D substitution was restored to wild-type tyrosine sequence with site-directed mutagenesis (Quickchange; Stratagene Inc., La Jolla, CA) utilizing the primers 5′-CGGCGGGATATAACATGAGCTGTCTTC-3′ and 5′-GAAGACAGCTCATGTTATATCCCGCCG-3′ (Biosource International, Camarillo, CA).

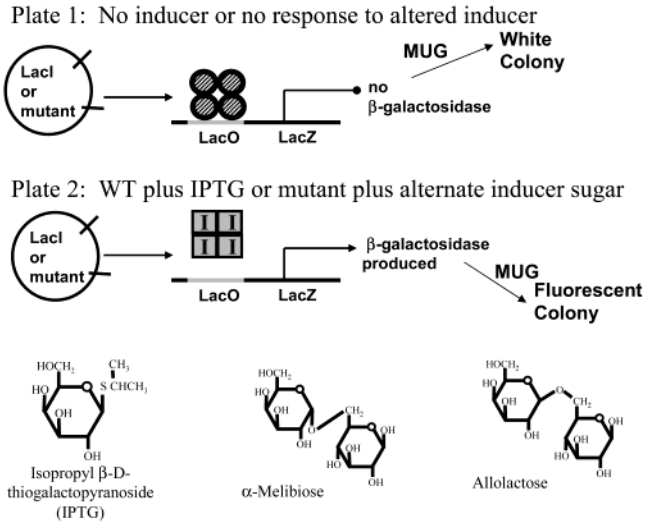

FIGURE 2: Schematic for the phenotypic screen for inducible repressor variants. The circle represents a plasmid containing the wild-type LacI sequence or a randomly mutated LacI gene. The phenotypic screen utilizes duplicate agar plates in the absence and presence of inducer. Two responses are possible. On the plate with no inducer, cells transformed with a LacI mutant that is capable of repressing the downstream *β*-galactosidase gene will produce white colonies in the presence of MUG (response 1). If this mutant protein is induced by one of the sugars in Table 1, colonies expressing that construct will fluoresce in the presence of MUG (response 2). Structures are shown for the inducers IPTG, α-melibiose, and allolactose at the bottom of the figure.

The double mutation Q60G/L148F was similarly created using the primers 5′-CTGGCGGGCAAAGGGTCGTTGCTGATTGGC-3′ and 5′-GCCAATCAGCAACGACCCTTTGCCCGCCAG-3′ (Genosys/Fisher; Houston, TX) to add the Q60G substitution to pCRE containing the L148F mutation. The coding regions of the DNAs containing all *lacI* mutations created by random or site-specific mutagenesis were fully sequenced (Genosys, Inc. or Lonestar Laboratories, Inc, Houston, TX) to confirm that they carried only the relevant substitutions.

Phenotypic Screening. Since the proteins in the extended LacI/GalR family (*2*, *15*, *30*−*32*) bind a range of small molecules (mono- and disaccharides, amino acids, ions, and nucleotides (e.g., refs *4*, *15*, and *33*−*36*), we anticipated that the LacI inducer binding site could be modified to recognize a different small molecule. Indeed, very recent studies accomplished a similar goal using the homologous periplasmic binding protein scaffold (*37*). The modified LacI would ideally retain both DNA binding/transcription control and the allosteric signal to relieve repression. Our experimental design was to couple random mutagenesis with a functional screen to identify variants with altered inducer specificity or with increased sensitivity to IPTG. Phenotypes of bacterial colonies expressing randomly mutated plasmids were ascertained using the screen shown in Figure 2 and adapted from Swint-Kruse et al. (*28*). Specific changes utilized the following: (i) *E. coli* 3.300 cells (see above) instead of DZCam (*28*), (ii) low copy pCRE plasmid instead of high copy pAC1 or pLS1, and (iii) the indicator 4-methylumbelliferyl *β*-D-galactopyranoside (MUG) as a fluorescent substrate of the reporter protein *β*-galactosidase instead of the

Table 1: Concentration of Sugars in LB Agar Plates for Phenotypic Screen of Randomly Mutated LacI

sugar	concentration (mM)[a]
IPTG	0.005
IPTG	0.25[b]
D-arabinose	100
L-arabinose	2.5
maltose	9
mannose	10
ribose	5
galactose	0.5
lyxose	10
α-melibiose	100

[a] Except for 0.25 mM IPTG, concentrations used in the screen were identified by finding the highest concentration of inducing sugar that did *not* induce wild-type LacI. Special care was taken to ensure that sugar concentrations were uniform between batches of plates. These included (i) carefully accounting for volume effects when making stock sugar solutions (which were stored in aliquots at −20 °C), and (ii) when pouring plates, waiting until agar was below 55 °C to add the sugar and ampicillin. The wide range of concentrations required for induction relates to a combination of affinity of the protein for the respective sugar and the efficiency of bacterial uptake and metabolism. The concentrations in vivo would be expected to differ significantly from the concentrations in the medium. [b] Control for IPTG quality; wild-type LacI should be induced under these conditions.

blue-white indicator 5-bromo-4-chloro-3-indolyl β-D-galactopyranoside (Xgal) (*38*). The first change increased reproducibility of the assay, whereas the latter adaptations increased sensitivity to induction through lowered repressor protein concentrations and enhanced detection of β-galactosidase activity.

Specifically, randomly mutated pCRE plasmid was transformed into $CaCl_2$-competent 3.300 *E. coli* and plated onto a variety of LB/agar/ampicillin plates with varied inducer sugars (Table 1). Plates were incubated overnight at 37 °C so that final colony diameters were ∼2 mm; smaller or larger colony sizes produced false negative or positive results. Next, a TLC sprayer was used to evenly spray the colonies with 20 mg/mL MUG in DMSO, and plates were viewed in UV light. Controls were provided by wild-type LacI, which should not produce fluorescent colonies in the absence of inducer, and the Y282D variant, which cannot repress transcription and thus should always exhibit fluorescent colonies. Fluorescent colonies of interest were replated in duplicate: (i) in the absence of inducer, to ascertain repressor function of mutated LacI and (ii) plus inducer, to reconfirm induction. Finally, the colony was grown in 5 mL of 2× YT broth for plasmid DNA purification (QIAprep Miniprep kit; Qiagen) and subsequent full sequencing. Two constructs with point mutations were identified, encoding the L148F and P320A substitutions. Surprisingly, both proteins appeared to be induced by the entire range of inducing sugars tested (Table 1).

Colony phenotype was further verified using a liquid culture β-galactosidase assay adapted from Miller (*38*). The only significant change was to use polymixin B to disrupt the cell membrane (16 μL of 2.5 mg/mL to a 5 mL culture) (*39*, *40*). Since repressor was expressed on a multicopy plasmid, β-galactosidase activity was not reproducible *between* colonies, and we could not reliably compare behaviors of different mutants. However, a single culture could be incubated in the presence and absence of various inducers to determine inducibility of a specific mutant repressor protein. Again, both L148F and P320A appeared to retain repressor function and to be induced by a wide range of sugars, including low concentrations of IPTG.

A number of double mutants identified by Swint-Kruse and co-workers (*28*) occur in a region of LacI structure near positions 148 and 320. Many of these mutations were tested with the β-galactosidase liquid assay for their inducibility. None were induced by alternate sugars. S151P/Y282D was chosen as a representative construct that had significant ability to repress and was induced by IPTG under the current screening conditions.

To verify intracellular concentrations of LacI L148F and P320A, whole cell extracts from 3.300 cells grown under conditions of the phenotypic screen were centrifuged to separate soluble protein from the cell pellet. Both soluble and pelleted samples were run in duplicate on 10% SDS−PAGE. One gel was stained for protein (either Coomasie or silver stain) and the other was used for Western blotting with a LacI polyclonal antibody (a gift from Jay Kirchner, Vanderbilt University). Results showed that significantly less soluble P320A was present in the cell extracts than either wild-type or L148F LacI.

Purification. Prior to purification, plasmids expressing the appropriate LacI mutations were transformed into chemically competent BLIM cells (*41*). After growing cells in 12 L of LB or 2× YT media overnight at 37 °C with shaking, cells were harvested by centrifugation. Before freezing the sample at −20 °C, a small amount of lysozyme was added to the resuspended cell pellet to facilitate lysis of bacterial cells. Most details of the purification were as described previously (*42*, *43*). The speed of purification was enhanced by changing the post-ammonium sulfate dialysis to three 30-min dialyses and buffer changes. Purified protein was divided into aliquots and stored at −80 °C. For high concentration protein samples used in spectroscopic studies, the eluate from phosphocellulose was dialyzed against buffer containing 0.05 M Tris-HCl, pH 7.4, 0.05 M KCl, 0.3 mM DTT overnight with one change of buffer. The protein was then loaded onto a heparin column using an FPLC system and eluted using a gradient composed of the loading buffer and an equal volume of 0.05 M Tris-HCl, pH 7.4, 0.5 M KCl, 0.3 mM DTT. The protein was concentrated using VIVASPIN20 at 2000*g* for approximately 2 h at 4 °C.

The S151P/Y282D double mutant did not purify similarly to tetrameric LacI and may be in equilibrium between various assembly states (monomer, dimer, tetramer). Therefore, we chose instead to study the singly substituted S151P repressor, which purified in the same manner as wild-type LacI. LacI containing L148F, Q60G/L148F, and P320A substitutions also purified like wild-type repressor. Gel filtration experiments using a Superose 6 column as part of a BioCAD 700E workstation (PerSeptive Biosystems, Framingham, MA) demonstrated that L148F, Q60G/L148F, S151P, and P320A all have a molecular mass of ∼150 kDa, comparable to wild-type LacI. Reference proteins included thyroglobulin (669 kDa), β-amylase (200 kDa), BSA (66 kDa), and cytochrome C (12.9 kDa). These experiments utilized 0.15−0.2 mg/mL LacI protein or variant, dialyzed into 200 mM Tris-HCl, pH 7.4, 200 mM KCl, 1 mM EDTA.

Stoichiometric DNA activity assays to measure the percentage of active protein were performed using a precisely known concentration of DNA at least 10-fold above the K_d

for DNA binding; a small fraction of radiolabeled DNA was used for detecting the amount of LacI·DNA complex retained on nitrocellulose filter paper (see below) (*44*−*46*). Activities of purified variants were generally >90%, and affinity binding constants determined under equilibrium conditions (with the concentration of DNA at least 10-fold below K_d; see below) and reported herein are corrected for activity.

Spectroscopy. A number of assays were used to determine mutant and wild-type protein concentrations and thus calculate $\epsilon_{280\ nm}$, including the BioRad Protein Assay (BioRad, Hercules, CA), magnetic circular dichroism determination of tryptophan concentration (Jasco J-500C spectropolarimeter attached to a 1.13 T electromagnet) (*47*), and the method of Edelhoch that employs guanidinium hydrochloride to denature protein so that the extinction coefficients of tryptophan and tyrosine residues approximate model compound values (*48*). Prior to concentration determination, centrifugation to remove any aggregated protein was essential for accurate measurements. For all mutants, $\epsilon_{280\ nm}$ appears to be the same as that of wild-type LacI, 0.6 $(mg/mL \cdot cm)^{-1}$ (*49*). However, L148F exhibited different behavior in the BioRad assay than wild-type protein, and the concentration of this protein must be determined by ultraviolet absorbance at 280 nm or one of the other methods indicated. All UV/visible spectroscopy was carried out using a Varian Cary 50 spectrophotometer.

UV difference spectra were determined for all mutants in the presence IPTG or α-melibiose. These experiments were performed at room temperature in 0.01 M Tris-HCl, pH 7.4, 0.15 M KCl using concentrations of 1.3−2 mg/mL protein and 1.0 mM IPTG or 10 mM α-melibiose prior to mixing. Protein and inducer solutions were centrifuged, and precisely equal volumes were added to separate sides of a split quartz cuvette. Absorbance was set to zero at 340 nm, and three spectra were recorded before and after mixing solutions in the cuvette. The step size was 0.25 nm with a 1 s average time. The difference spectrum was determined by subtracting the average spectrum of apoprotein from the average ligand-bound spectrum.

Fluorescence spectroscopy was performed using either an SLM-Aminco AB2 or an SLM-Aminco 8100 spectrofluorometer using an excitation wavelength of 285 nm and recording fluorescence spectra from 300 to 380 nm. Protein concentration was ∼0.05 mg/mL following dialysis into 0.01 M Tris-HCl, pH 7.4, 0.15 M KCl. Circular dichroic spectra were obtained at room temperature on an AVIV 62DS spectropolarimeter. Spectra derived were an average of three scans collected from 200 to 250 nm with a 0.25-nm step size and a 1 s average time; protein concentration was ∼0.5 mg/mL in 0.12 M potassium phosphate, pH 7.4.

DNA Binding. Stoichiometric (activity) and equilibrium (affinity) DNA binding to LacI mutants was monitored by nitrocellulose filter binding assays (*44*−*46*). Oligonucleotides encoding the 40-base natural operator O^1 (5′-TGTTGTGTGGAATTGTGAGCGGATAACAATTTCACACAGG-3′) (*50*) were purchased from Biosource International (Camarillo, CA). The top and bottom strands were hybridized (70 mM Tris-HCl, pH 7.6, 10 mM $MgCl_2$, 5 mM DTT) and radiolabeled at the 5′ end using [^{32}P]-ATP via a polynucleotide kinase reaction. To purify labeled operator from free nucleotide, the reaction mixture was passed through a Nick column (Amersham Biosciences, Uppsala, Sweden). For the equilibrium assay, DNA concentration was set at least 10-fold below the lowest K_d estimated for operator binding, and protein concentration was varied. Protein concentrations and buffers are indicated in the table footnotes and figure legends. After filtration on nitrocellulose (Schleicher and Schuell, Keene, NH), protein-bound, radiolabeled DNA was detected and quantified using a Fuji phosphorimager. Data (Y_{obs}) were analyzed with IgorPro (Wavemetrics, CA) or NonLin (*51*) to estimate values for the variables in the following equation:

$$Y_{obs} = Y_{max}\frac{[LacI]^n}{K_d^n + [LacI]^n} + c \qquad (1)$$

Here, Y_{max} is the level of radioactivity measured when 100% of the DNA was in complex with repressor, K_d is the equilibrium dissociation constant, and c is the level of background radioactivity detected when no DNA is bound to repressor. The value n was either fixed at 1 or allowed to float, in which case the values cluster around 1.

IPTG Binding. Inducer binding to LacI mutants was monitored using fluorescence emission intensity change with increasing concentrations of IPTG (*52*). Experiments utilized a 340 nm cutoff filter (O-52) from Corning with an excitation wavelength of 285 nm. Total LacI fluorescence above 340 nm decreases upon the addition of inducer. Protein concentration was set so that it was at least 10-fold below the K_d determined for inducer binding, and IPTG concentration was varied. Inducer concentrations and buffers are indicated in the table footnotes and figure legends. An identical titration, using buffer instead of inducer, was performed for each experiment to correct for effects of photobleaching and dilution (*53*). Corrected data (Y_{corr}) were analyzed with the following equation:

$$Y_{corr} = Y_{max} - \left(Y_{max}\frac{[IPTG]^n}{K_d^n + [IPTG]^n}\right) + c \qquad (2)$$

Equation 2 is a variation of eq 1 that accommodates decreasing signal as a function of inducer binding. The program Igor Pro (Wavemetrics, CA**)** or NonLin (*51*) was used to determine values for the four variables: Y_{max}, the maximum change in fluorescence signal between conditions of zero and saturating inducer; n, the Hill coefficient; K_d, the apparent equilibrium dissociation constant; and c, a constant background coefficient. For inducer binding, the wild-type value of n is 1 in the absence of operator, but increases to ∼1.5−1.9 in the presence of operator DNA (*53*, *54*). Therefore, n was allowed to float during the fitting process, but for all mutant proteins this value clustered around 1 in the absence of operator DNA. When presented in the figures, these data are recast as fraction bound, which increases with inducer concentration.

Operator Release. These experiments measure the concentration of inducer sugar needed to release operator from the LacI·DNA complex. We utilized two different experimental designs: (i) The concentration of radiolabeled DNA was set ≥10-fold below K_d, as in operator binding experiments (10^{-13}−10^{-12} M), whereas the repressor concentration was such that ∼80% of the operator was bound (*53*); (ii) the concentration of DNA ($1.5-2 \times 10^{-8}$ M) was set 3-fold higher than the concentration of protein ($5-7 \times 10^{-9}$ M), so that all repressor protein was bound to operator. Note,

however, that the DNA concentration remained below the K_d for LacI·inducer binding to DNA. In both types of experiments, the concentration of inducing sugar was varied, usually in the range of $10^{-8}-10^{-3}$ M. Because the inducer concentration in both types of experiment was in vast excess of the protein, the same phenomenon was monitored, even though design (i) included unbound LacI. Similar results were obtained for these two experimental conditions, and results from arrangement (i) are shown in Figure 5. Data were quantitated with a Fuji phosphorimager and analyzed with eq 2. In this instance, K_d does not represent a true equilibrium constant and can be thought of as $[\text{inducer}]_{mid}$. In contrast to fluorescence-detected inducer binding, which observes the event of one repressor monomer binding one inducer molecule (*53*, *55*), operator release monitors at least two events: (i) binding the number of inducer molecules required to release DNA (an unknown number) and (ii) the accompanying protein conformational change.

Urea Denaturation. Urea denaturation experiments were carried out as previously described (*56*, *57*). Denaturation was monitored by changes in fluorescence intensity at 340 nm, and data were analyzed to identify the midpoint of the transition for comparison with wild-type operator. Urea denaturation is fully reversible for wild-type LacI (*57*) and all variant proteins.

RESULTS

Core Pivot Region. The core pivot of the LacI core domain is defined as the central portions of the three strands that interconnect the N- and C-subdomains of the LacI core (amino acids 161−164, 290−293, and 318−322) (*23*). Two additional loops contact this region, further involving amino acids 150−153 and 190−193. Since the core pivot area is near the back of the inducer-binding pocket (Figure 1A), the functional phenotypes of mutations in this region were previously interpreted as important to inducer binding if they resulted in the inducer-insensitive phenotype (I^s), whereas those exhibiting loss of repression (I^- phenotype) were generally thought to be requisite for maintaining structural integrity (i.e., these mutants did not fold or assemble properly) (*58*, *59*). Recently, a number of mutations were identified in or adjacent to the core pivot region by their ability to restore repression to the I^- phenotype of Y282D (at positions 133, 149, 150, 151, 191, 296, and 321) (*24*). The Y282D variant of LacI is monomeric and thus lacks an intact high-affinity DNA binding site formed by the two N-terminal domains of a dimer. However, the core domain of Y282D retains wild-type inducer-binding affinity and thus must retain the native fold. Therefore, these new substitutions were postulated to have a long-range conformational effect on the structure, with possible consequent changes in the LacI allosteric mechanism (*24*).

Recently, the core pivot region has been implicated as a crucial part of the allosteric conformational change by analysis of a TMD simulation (*23*). These observations support previous hypotheses regarding the Y282D long-range revertants. In addition, we have recently identified two new mutations in this region (L148F and P320A) via phenotypic screen for changed inducer properties (see Materials and Methods, above). We have therefore directly explored the possibility of long-range, allosteric, structural effects of these core pivot substitutions. We report the identification, purification, and initial biochemical characterizations of L148F, P320A, as well as purification and characterization of S151P (originally identified in the Y282D revertant screen). We have also used site-specific mutagenesis to create the Q60G/L148F double mutant, which was characterized in parallel with the other three LacI variants. The double mutant provides an opportunity to determine the interactivity of mutations in distinct domains that individually enhance binding of opposing ligands (DNA versus inducer) (*25*). In addition, the resulting variant with full repression and greater sensitivity to inducer may potentially be substituted for wild-type LacI in technological applications to reduce the cost of induction.

Phenotypic Screen. Thousands of LacI single-site substitutions have been catalogued by their phenotype (e.g., refs *38*, *58*, *60*, and *61*). These data are enormously informative, but this method is limited to reporting phenotypic differences resulting from a *loss* in either the repression or induction function. Previously, we developed a screen to detect gain of repression for second-site reversion mutations of the LacI Y282D mutant (*28*). Here, we report a new adaptation that detects LacI mutants with altered inducer properties. We screened ∼50 000 colonies expressing random mutants in this study. We detected two point mutations that satisfied our phenotypic criteria, L148F and P320A.

Both L148F and P320A were induced by all sugars tested in plate and liquid culture assays of β-galactosidase activity, including IPTG levels 10-fold less than the lowest concentration required to induce wild-type. For P320A, this phenotype is fully consistent with the previous study showing no loss of repression or induction for this substitution (*58*). Although phenylalanine substitution at position 148 was not explored in earlier genetic studies, other substitutions at position 148 exhibit partial or full loss of repression (*58*), consistent with biochemical analysis of L148F (see below). Western blot analysis of protein levels in the 3.300 cells indicated these cells expressed ∼2-fold less soluble P320A than either wild-type LacI or L148F variant, which were expressed at comparable levels (data not shown).

In light of their structural proximity, we also monitored the inducer phenotypes of several long-range revertants of Y282D—including D149N, V150I, S151P, and V321I (*28*). Experiments were performed using both the double (revertant plus Y282D) and single mutations (reversion mutation in a wild-type background). None of these mutants were induced by other sugars (data not shown). However, preliminary biochemical evidence indicated that the S151P single mutant had DNA and inducer binding properties *opposite* to those of L148F. Therefore, we continued characterization of this LacI mutant.

Purification and Characterization of Core Pivot Mutations. Determination of the phenotype caused by a protein variant can be very useful. However, multiple functional changes may combine to effect a given behavior in vivo. The phenotypes generated in *E. coli* may result from changes in any combination of (i) inducer specificity, (ii) inducer affinity, (iii) protein expression levels, (iv) repressor stability, (v) DNA binding affinity, (vi) the ratio between LacI conformations with different properties (e.g., the T and R states described by Monod-Wyman-Changeux analysis), or (vii) metabolism of alternate sugars that results in induction

Table 2: DNA Binding by LacI Core Pivot Mutations[a]

	K_d (M × 10^{11})	mutant/WT
WT	1.5 ± 0.43	1
L148F	49 ± 15	33
S151P	0.48 ± 0.05	0.32
P320A	0.40 ± 0.19	0.27
Q60G/L148F	4.6 ± 1.6	3.1
Q60G[b]	0.38 ± 0.07	0.25

[a] Operator binding was measured in buffer containing 0.01 M Tris-HCl, pH 7.4, 0.15 M KCl, 0.3 mM DTT, 0.1 mM EDTA, 5% DMSO. Operator concentration was less than 1.5×10^{-12} M for L148F, WT, and Q60G/L148F proteins, and less than 1.5×10^{-13} M for P320A, S151P, and Q60G proteins. Standard deviations shown represent a minimum of three measurements and up to six measurements. [b] Originally reported in ref *25*.

by unspecified molecules. Biochemical analysis of purified protein is critical to determining exactly which processes are affected. All four LacI mutants (L148F, S151P, P320A, and Q60G/L148F) purified in a manner similar to tetrameric wild-type protein. This process is sensitive to oligomerization state (*42*, *54*, *62*), and gel filtration demonstrated that all exhibit the molecular weight anticipated for tetrameric protein, ~150 kDa (*42*, *54*, *62*). Further characterization included UV/visible and fluorescence spectroscopy, circular dichroism spectropolarimetry, determination of thermodynamic parameters for operator and inducer binding, and urea denaturation. Results are presented in subsequent sections and summarized in Tables 2−4.

Spectroscopy. Data from a variety of techniques to establish protein concentration demonstrate that all purified repressor variants have the same extinction coefficient at 280 nm (see Materials and Methods). Fluorescence spectra were determined for the purified L148F, P320A, S151P, and Q60G/L148F substitutions of LacI. Compared to wild-type protein, the quantum yields of all the mutant proteins are very similar (data not shown). Since the tryptophan residues (positions 201 and 220) that dominates LacI fluorescence are not in close proximity to the core pivot (*7*, *20*, *49*), this similarity is not surprising. Circular dichroism spectroscopy demonstrates that the mutant proteins exhibit spectra similar to wild-type LacI (data not shown), consistent with their fluorescence spectroscopic properties and ability to purify similarly to the wild-type protein. The folding pattern of the mutant proteins does not appear to be disrupted by the substitutions introduced.

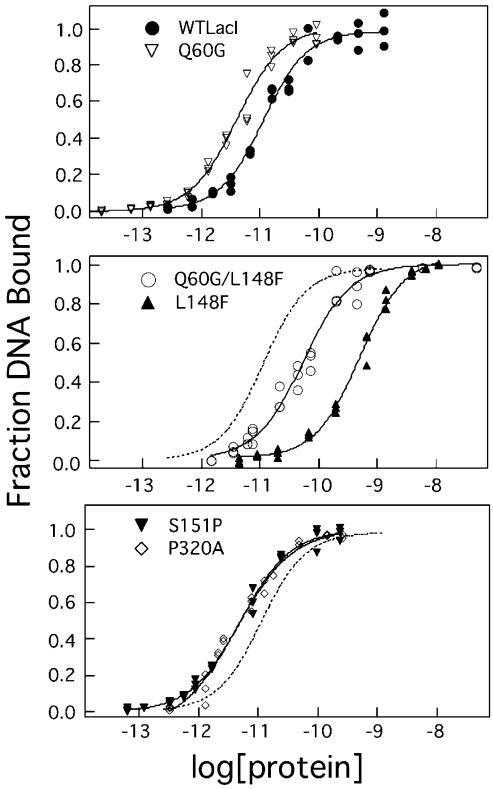

FIGURE 3: Operator DNA binding of LacI variant proteins. Operator binding assays were conducted as described in Materials and Methods. Binding at each of the indicated protein concentrations was measured in buffer containing 0.01 M Tris-HCl, pH 7.4, 0.15 M KCl, 0.3 mM DTT, 0.1 mM EDTA, 5% DMSO. Operator concentration was less than 1.5×10^{-12} M for L148F, WT, and Q60G/L148F proteins, and less than 1.5×10^{-13} M for P320A, S151P, and Q60G proteins. Data are shown for single determinations (triplicate points). Data were analyzed as described in Materials and Methods, and the results from multiple determinations are summarized in Table 2. The dashed line in the lower two panels is the fitted curve for wild-type LacI for comparison.

DNA Binding. Operator affinity was determined for each mutant using the nitrocellulose filter binding technique (Table 2; Figure 3) (*44*−*46*). The data demonstrate that mutations in the core pivot can either strengthen or weaken DNA binding affinity: L148F binds DNA >30-fold more weakly than wild-type repressor, while P320A and S151P bind operator at least 3-fold more tightly. The Q60G mutation was previously discovered to increase operator binding

Table 3: Inducibility of LacI Core Pivot Mutations[a]

	inducer binding[b]			operator release[c]		
	K_d (M × 10^6)		mutant/WT	$[inducer]_{mid}$ (M × 10^6)		mutant/WT
	α-melibiose	IPTG	IPTG	α-melibiose	IPTG	IPTG
WT	160 ± 31	1.2 ± 0.13	1	460 ± 190	2.9 ± 0.62	1
L148F	260 ± 38	0.41 ± 0.07	0.34	370 ± 190	0.71 ± 0.08	0.24
S151P	1600 ± 150	4.5 ± 0.8	3.8	2200 ± 800	6.9 ± 1.3	2.4
P320A	210 ± 15	1.0 ± 0.2	0.83	380 ± 340	3.1 ± 1.8	1.1
Q60G/L148F	250 ± 5.5	0.40 ± 0.08	0.33	290 ± 240	0.80 ± 0.25	0.28
Q60G[d]	180 ± 17	1.5 ± 0.3	1.3	500 ± 300	2.9 ± 1.1	1.0

[a] Standard deviations shown represent a minimum of three measurements and up to six measurements. [b] Sugar binding was measured in buffer containing 0.01 M Tris-HCl, pH 7.4, 0.15 M KCl by fluorescence spectroscopy as described in Materials and Methods. Protein concentration was below 5×10^{-7} M monomer for α-melibiose and below 1.5×10^{-7} M monomer for IPTG measurements. [c] Operator release was monitored in buffer containing 0.01 M Tris-HCl, pH 7.4, 0.15 M KCl, 0.3 mM DTT, 0.1 mM EDTA, 5% DMSO. Operator concentration was 1.5×10^{-12} M, and protein concentrations were as follows: wild-type, 2.4×10^{-10} M; L148F, 6.5×10^{-9} M; S151P, 9.6×10^{-11} M; P320A, 1.1×10^{-10} M; Q60G/L148F, 6.5×10^{-10} M; Q60G, 5.2×10^{-11} M. Alternatively, operator was $(1.5-5) \times 10^{-8}$ M, protein $(5-7) \times 10^{-9}$ M. Both experimental designs yielded similar values (see Materials and Methods). [d] Originally reported in ref *25*.

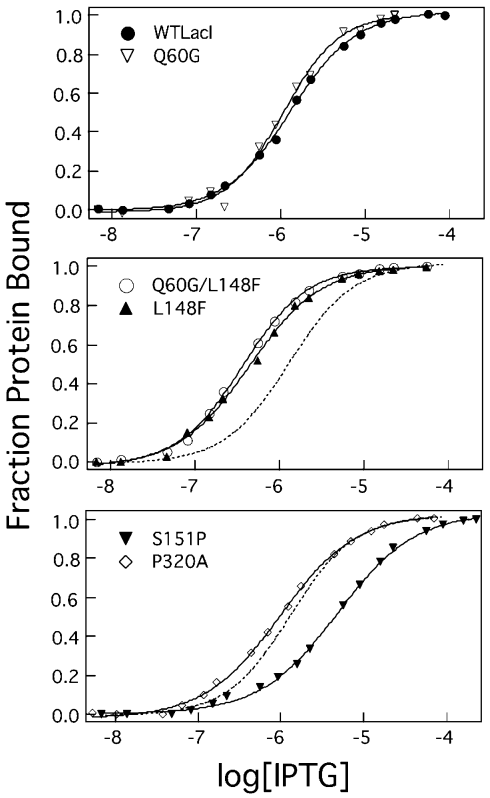

FIGURE 4: IPTG binding of LacI variant proteins. IPTG binding was measured by fluorescence spectroscopy as described in Materials and Methods. Protein was diluted into buffer containing 0.01 M Tris-HCl, pH 7.4, 0.15 M KCl. Final protein concentration was below 1.5×10^{-7} M monomer. Data shown are for single titrations for each of the proteins, and the results from multiple analyses are summarized in Table 3. The dashed line in the lower two panels is the fitted curve for wild-type LacI for comparison.

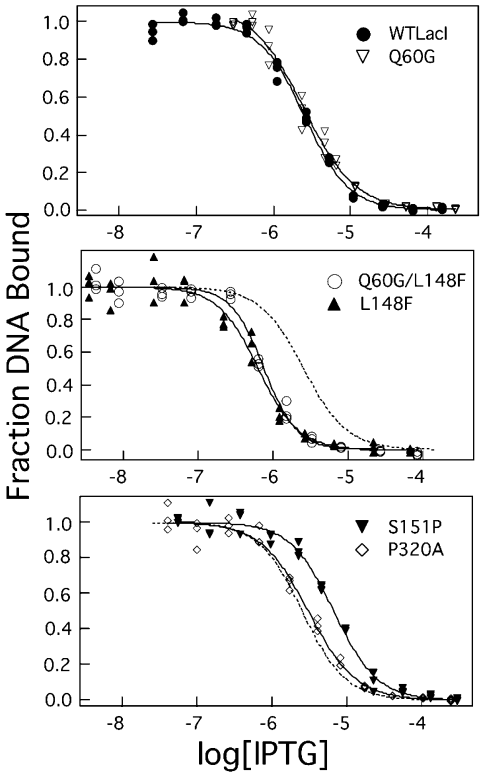

FIGURE 5: Operator release by IPTG for LacI variant proteins. Protein complexed to operator was exposed to varying concentrations of IPTG to monitor release. These experiments were performed as described in Materials and Methods in buffer containing 0.01 M Tris-HCl, pH 7.4, 0.15 M KCl, 0.3 mM DTT, 0.1 mM EDTA, 5% DMSO. In the experiments shown, operator concentration was 1.5×10^{-12} M, and protein concentrations were as follows: wild-type, 2.4×10^{-10} M; L148F, 6.5×10^{-9} M; S151P, 9.6×10^{-11} M; P320A, 1.1×10^{-10} M; Q60G/L148F, 6.5×10^{-10} M; Q60G, 5.2×10^{-11} M. Data from a single experiment (triplicate points) are shown, and the results from multiple measurements are summarized in Table 3. The dashed line in the lower two panels is the fitted curve for wild-type LacI for comparison with the variants.

affinity nearly 4-fold (*63*). When combined with the L148F mutation, the $K_{d,DNA}$ for the double mutant was increased ~10-fold over that of the single core pivot substitution. None of the DNA binding data for the mutants reflected evidence of coupled protein assembly and DNA binding, consistent with other data that indicates tetrameric structure.

Inducer Binding. Although allolactose (Figure 2) is the natural inducer of LacI (*64*), a number of other compounds can serve as gratuitous inducers (*36*, *64*). Of these, IPTG is bound most tightly, with a micromolar equilibrium dissociation constant (*65*). L148F and P320A were isolated because, based on phenotype, they can be induced by a variety of sugars. Although the sugars presented in Table 1 were able to serve as inducers in vivo, only IPTG and α-melibiose were effective inducers in DNA binding assays in vitro using purified proteins (data not shown). L-Arabinose and galactose at 1 mM elicited a small decrease in operator binding in the in vitro assays for L148F and Q60G/L148F (~20%), compared to a smaller effect (~10%) of arabinose on wild-type protein and P320A. Galactose had no effect on wild-type LacI or P320A.

Inducer binding affinity for LacI and its mutants can be determined by monitoring the change in repressor fluorescence as a function of sugar concentration (*53*). Data from these experiments indicate that alterations in the core pivot can affect IPTG binding in a manner *opposite* to changes in operator affinity: L148F binds IPTG 3-fold more tightly than wild-type, whereas S151P binds nearly 4-fold less tightly (Table 3, Figure 4). Q60G/L148F retains the inducer binding affinity of the single L148F substitution. Interestingly, P320A has very little influence on IPTG affinity, a result that suggests this mutation may engender its DNA binding enhancement through a mechanism distinct from that for L148F and S151P. One possibility is that the proline to alanine mutation increases flexibility in the core pivot region. Future experiments will explore this possibility by monitoring binding kinetics.

α-Melibiose is a disaccharide and isomer of the natural inducer allolactose (Figure 2). Despite the fact that its K_d (~10^{-4} M) is 100-fold less than that of IPTG, α-melibiose is bound by wild-type LacI with higher affinity than most other known inducers (*65*, *66*). Fluorescence spectroscopy was used to monitor α-melibiose binding to wild-type LacI, and results were in agreement with previous equilibrium dialysis experiments (Table 3) (*65*). Interestingly, similar affinity for this ligand was observed for all of the mutants except S151P, which exhibited a greater decrease (almost 10-fold) for α-melibiose affinity relative to wild-type than for IPTG (~4-fold). Thus, the mutated residues in the core pivot region interact differently with alternate inducer sugars.

Operator Release. Even though a LacI variant may be able to bind both operator and inducer, allosteric communication

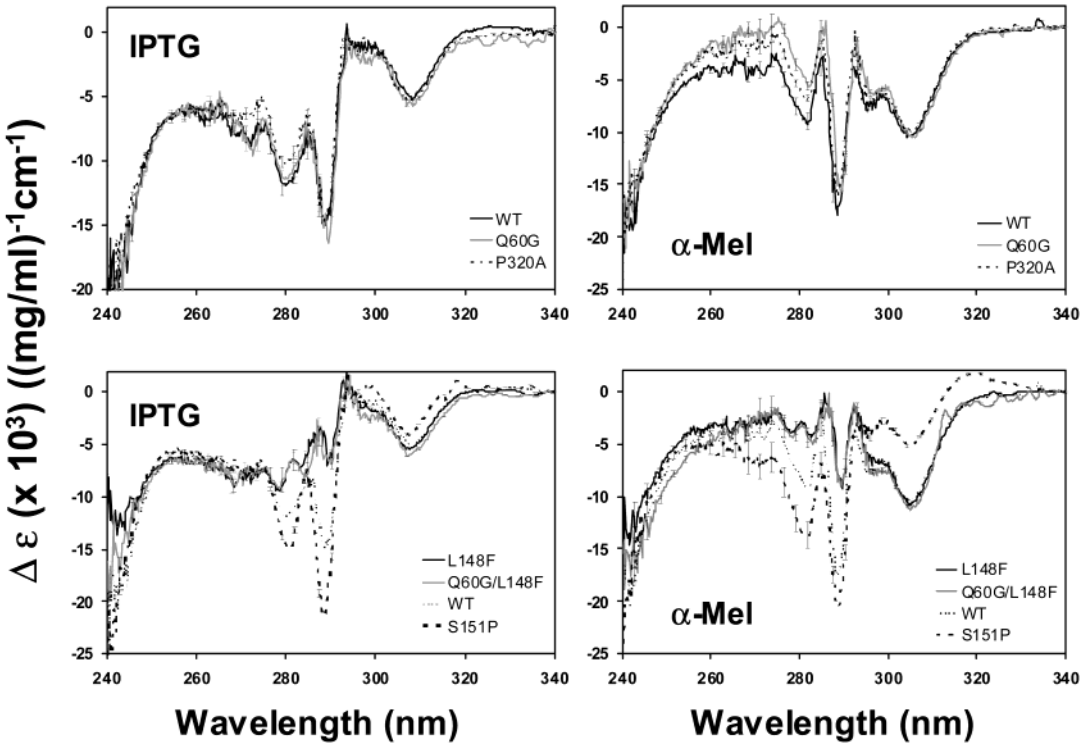

FIGURE 6: UV difference spectra in response to IPTG and α-melibiose. Difference spectra were measured as described in Materials and Methods at room temperature in buffer containing 0.01 M Tris-HCl, pH 7.4, 0.15 M KCl. Protein (~30 mg/mL) was diluted to 1.3−2 mg/mL into buffer prior to spectral measurements. Protein was placed in one chamber of a split quartz cuvette, and a precisely equal volume of 1.0 mM IPTG or 10 mM α-melibiose was added to the other chamber. After mixing, the final concentrations of inducer and protein were precisely half their initial concentrations, while the effective path length for the mixed solution doubled. The spectra are reported as the change in the absorption coefficient. The difference spectra were determined by subtracting the average of three spectra for the unmixed, apoprotein from the average of three spectra for the mixed, inducer-bound protein. Error bars are shown for every fifth data point; the width of the error bars is frequently similar to the width of the plotted spectrum. In the lower panels, the wild-type spectra are repeated for comparison with the LacI variant proteins; wild-type error bars were not repeated for simplicity.

between the two sites can be altered or disrupted (*43*). Operator release experiments monitor the concentration of inducer required to release radiolabeled DNA from a complex with repressor protein. We employed filter binding to monitor this process using IPTG and α-melibiose as inducers. Results are presented in Table 3 and Figure 5. For wild-type LacI, our data compare very well with values reported in the literature (*36*, *44*). Data for both sugars correlate with repressor affinity for that compound: L148F and Q60G/L148F release operator at lower IPTG concentrations; S151P requires more IPTG; and P320A behaves similarly to wild-type LacI. For α-melibiose, L148F, Q60G/L148F, and P320A behave similarly to wild-type protein, and S151P requires more α-melibiose. In fact, the wild-type-to-mutant ratios for K_d and $[sugar]_{mid}$ are essentially identical for all repressor mutants.

UV Difference Spectroscopy. To explore the effects of inducer binding on the structure of the protein, UV difference spectra were measured for IPTG and α-melibiose binding to the variant proteins (Figure 6). Q60G, S151P, and P320A exhibited spectra similar to wild-type LacI for both IPTG and α-melibiose binding, although the minima at 278 and 288 were consistently deeper for S151P. However, L148F and Q60G/L148F exhibited spectra substantially different from the other proteins in the 275−295 nm region. Furthermore, the difference spectra were very different for IPTG and α-melibiose, paralleling more subtle differences between these sugars previously observed for wild-type protein and mutants with single tryptophans (*49*). These data suggest that occupation of the inducer binding site elicits a quite different set of structural changes in proteins with the L148F mutation and that variant sugars may trigger conformational shifts that affect aromatic residues differently. These changes appear to alter spectral regions that can be ascribed to both tyrosine and tryptophan absorption and are thus dispersed in the structure rather than localized.

Urea Denaturation. Analysis of LacI function is very complex. In addition to binding two different ligands and undergoing an allosteric change between two conformations, thermodynamic linkage to repressor assembly and folding equilibria must also be taken into account. Thus, functional effects of mutations can indirectly result from altering structural equilibria. Urea denaturation experiments can assess whether these latter processes are affected by side-chain substitution (*56*, *57*). Although rigorous thermodynamic analysis is complicated by the linked equilibria, comparison of denaturation midpoints provides a simple means of comparing LacI variants and identifying targets for detailed future studies. Repressors containing L148F and S151P substitutions are more sensitive than wild-type LacI to urea denaturation, while P320A and Q60G appear to be unaltered (Figure 7 and Table 4). These results suggest that the L148F and S151P substitutions exert long-range structural effects on the repressor structure. However, recall that S151P was discovered by its ability to restore repressor function to the monomeric Y282D mutant, presumably through restoration of assembly. Thus, S151P may alter the monomer−monomer interface, and the alternate interface may be less stable to

Table 4: Urea Denaturation of LacI Core Pivot Mutations[a]

	$[urea]_{mid}$ (M)
WT	2.8 ± 0.1
L148F	2.3 ± 0.1
S151P	2.6 ± 0.1
P320A	2.8 ± 0.1
Q60G/L148F	2.4 ± 0.2
Q60G	2.8 ± 0.1

[a] Urea denaturation was measured in buffer containing 0.01 M Tris-HCl, pH 7.4, 0.1 M K_2SO_4 with protein concentration at 2×10^{-6} M monomer as described previously (*56*, *57*). Standard deviations shown represent a minimum of three measurements and up to six measurements.

urea denaturation. Experiments are in process to explore these possibilities further.

DISCUSSION

When LacI changes from the DNA- to inducer-bound conformation, the core C-subdomains anchor the screwing motions of the N-subdomains (*6*, *67*). When comparing the two crystal structures, interest has focused on the N-subdomain interface, which is subject to widespread rearrangement. In contrast, the core pivot region that interconnects the N- and C-subdomains shows little alteration between these static views. In fact, the leucine side chain of 148 undergoes very little change between the operator- and inducer-bound LacI X-ray crystallographic structures (*6*, *7*); the leucine moves as a unit with the N-subdomain, but all of the residues contacted by 148 remain within 0.5 Å of their original juxtapositions (Table 5). Likewise, the serine 151 side chain shows only subtle variations, and the side chain of proline 320 is solvent exposed and shows almost no change between the two structures (*6*, *7*; Table 5). Recently, however, TMD has implicated the core pivot region as structurally important to the conformational change (*23*). Around the same time, phenotypic selection of randomly generated mutants suggested that this region has a crucial role in LacI function (reported herein and in ref *24*).

This manuscript reports biochemical analysis of core pivot variants that integrates information from TMD and phenotypic analysis. Despite the effectiveness of broad scale mutagenesis and in vivo phenotypic analysis, the present work illustrates the importance of biochemical analysis of purified proteins in understanding the behavior of any identified mutants. For example, P320A exhibited an identical phenotype to L148F, an observation that persisted through multiple rounds of screening in both plate and liquid assays. Nevertheless, purified P320A protein demonstrates no change in inducibility or inducer binding and paradoxically exhibits increased operator binding affinity, whereas the biochemical behavior of L148F is easily reconciled with its phenotype. The apparent discrepancy between phenotypic and biochemical analyses for P320A likely arises from its lowered protein expression levels, a situation masked by its enhanced affinity for operator DNA. Thus, fewer P320A repressor proteins adequately repress the reporter gene, and the increased inducer/protein ratio might appear as greater inducer sensitivity.

At first glance, the binding parameters presented in Tables 2−4 appear to provide a simple structural explanation for the biochemical behaviors of L148F and S151P. Since the DNA and IPTG affinities of these mutants change in a seesaw manner, the most obvious explanation is that these mutations change the allosteric constant L, the ratio between the populations of the two allosteric conformations R and T in the Monod-Wyman-Changeux model. For unliganded wild-type LacI, both conformations are equally populated. Thus, the allosteric constant is ~1 (*53*, *55*), the $\Delta G_{conformation}$ is zero, and the measured DNA and inducer K_d values reflect intrinsic binding affinities (*53*). However, if an amino acid substitution changes L, $\Delta G_{conformation}$ is nonzero and contributes to the free energies of DNA and IPTG binding in opposite manners (e.g., ref *68*). The hypothesis of a changed allosteric constant is consistent with the structural role of the core pivot (Figure 1A). Further, the close parallel between inducer binding and operator release experiments indicates that none of the core pivot mutations alters the basic mechanism of allosteric communication in LacI. Additional experiments will be required to determine the allosteric constant, L, for each mutant and construct complete thermodynamic circuits for these proteins to directly test this possibility (*53*, *55*).

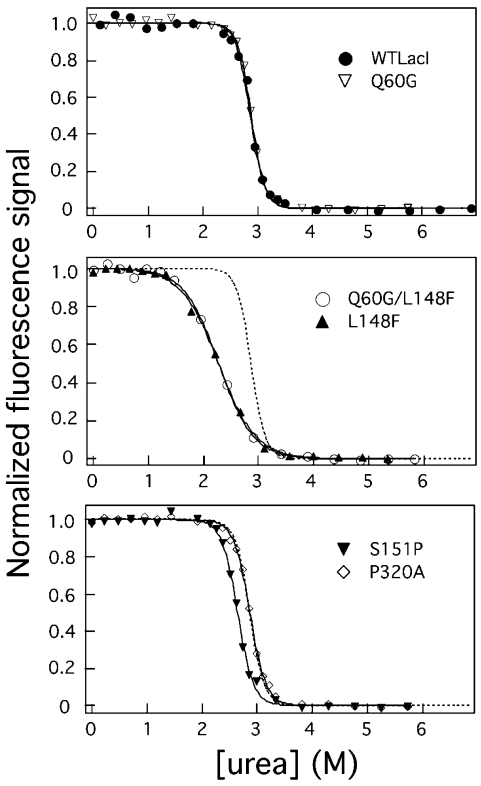

FIGURE 7: Urea denaturation of LacI core pivot variants. Urea denaturation was performed as described in Materials and Methods. Data from single experiments are shown, and the results from multiple measurements are summarized in Table 4. Solid lines are the results from fitting to an equation modeling denaturation of a single domain, monomeric protein and thus are only intended to aid visual inspection/normalization of the data. The dashed line in the lower two panels is the fitted curve for wild-type LacI, which is repeated for comparison with the variants.

The effects of L148F and Q60G on repressor function appear largely to be additive and independent rather than synergistic. The properties of L148F binding dominate all features of inducer binding for the Q60G/L148F double mutant, as well as its structural changes reflected in UV difference spectroscopy and urea denaturation. If L148F functional effects were derived from a drastically altered

Table 5: Contacts between Sites of Core Pivot Mutations and Residues of Allosteric Pathways in Wild-Type LacI[a]

	contacts	distance (Å)[b]	movement (Å)[c]	allosteric participation pathway: structural region[d]
L148	I83*[e]	4.9	−0.5	1: N-subdomain hydrophobic
	I123*	3.9		1: N-subdomain hydrophobic
	L146*	4.5	−0.5	1: N-subdomain hydrophobic
	D149*	1.3		1: flexible loop
	V150	3.7	−0.4	1: flexible loop
	L296*	4.1		3: core pivot hydrophobic
S151	V150*	1.3		1: flexible loop
	D152*	1.3		1: flexible loop
	Q153*	2.9	−0.5	1: flexible loop
	T154*	3.1	−0.4	1: flexible loop
P320	F161*	3.5		3: core pivot hydrophobic
	L295*	4.6		3: core pivot hydrophobic
	L319*	1.3		3: core pivot hydrophobic
	V321*	1.3		3: core pivot hydrophobic

[a] Contacts are listed for polar/charged amino acids within 3.5 Å of the designated core pivot mutation in the DNA-bound structure of wild-type LacI (1efa) (*6*) or for hydrophobic residues within 5 Å. Contact residues were identified using the web-based program Contacts of Structural Units (http://bioinfo.weizmann.ac.il:8500/oca-bin/lpccsu) (*73*). [b] Shortest distance between the site of the core pivot mutation in the repressed form of wild-type LacI (1efa) (*6*); calculated with CSU (*73*). [c] Distance between core pivot mutation site and residue changes by ≥0.4 Å upon the conformational change from the repressed (1efa) (*6*) to the induced form (1lbh) (*6*). [d] The numbers represent the pathway in which the partner amino acid participates during the allosteric transition; the structural region is also described (*23*). [e] Asterisk (*) indicates contacts made through partner side chain.

protein conformation, a likely consequence would be to change the orientation of the core N-subdomain with consequent interruption of the interface between the top of the subdomain and the DNA binding domain. Note, however, that Q60G is located in this interface. This mutation has a similar functional effect on both wild-type and L148F LacI (i.e., enhancing DNA binding) (*25*), although the enhancement in the L148F background is slightly higher than that in the wild-type LacI context. Therefore, the interface appears to be intact in the double mutant. Together, these observations support the interpretation that L148F shifts the population between normally accessible states rather than generating a new conformation(s).

However, at least one observation conflicts with the allosteric model. Note that L148F and Q60G/L148F affinity for the alternate inducer α-melibiose does *not* change, yet this compound fully induces these mutant repressors. These data can be reconciled if α-melibiose and IPTG trigger the LacI allosteric conformational change via distinct mechanisms. In fact, UV difference spectra for LacI in the presence and absence of inducer differ for IPTG and α-melibiose (*49*). This distinction is more pronounced for L148F and Q60G/L148F than for the other proteins examined (Figure 6) and is intriguingly reminiscent of the behaviors for a family of LacI variants that have allosteric properties dependent upon the sequence of DNA bound (*69*, *70*).

Biochemical analysis also offers several avenues for understanding how the S151P mutation, with its enhanced affinity for operator and diminished affinity for inducer, might compensate the assembly defect of the Y282D substitution, the manner in which this mutant was originally isolated. First, increased operator affinity of S151P might allow otherwise undetectable levels of Y282D oligomer to exert detectable repression function. Alternatively, urea denaturation experiments indicate that the stability of the monomer−monomer interface or the stability of the core domain is altered in S151P. Perhaps this core pivot mutation reorients the N-subdomain so that a new monomer−monomer interface is formed that can better accommodate Y282D effects in the C-subdomain. Preliminary attempts to crystallize this protein have been successful, and we hope a structure will be forthcoming that can illuminate structural differences with wild-type LacI.

Finally, since DNA binding of P320A is affected independently of the inducer-binding affinity, results do not suggest a change in L for this variant. Instead, the conversion of proline to alanine significantly alters backbone constraints in a region where flexibility is crucial (see legend to Figure 1A (*23*)). This possibility is easily reconciled with the TMD results (*23*), which demonstrate that the backbone ϕ and ψ angles of the interconnecting strands (which encompass P320) change over the course of the allosteric transition. This change may lower the energy barrier to the conformational shift in response to inducer. More detailed thermodynamic and kinetic experiments will illuminate the possibilities.

Analysis of the TMD simulation indicated that motions that drive the allosteric change could be grouped into three pathways that intersect at the core pivot and the core N-subdomain interface (Figure 1A). While neither L148 nor S151 directly participates in these processes, collectively positions 148, 151, and 320 contact a large number of residues that undergo significant changes (Table 5). Partners to 148 participate in pathways 1 and 3, so changes at L148 could potentially affect both processes. Further, the leucine at position 148 contacts residues I70 and D149 that interact with IPTG, and L148 itself may have some hydrophobic interaction with ligand (*6*, *7*, *20*). S151 is located on a flexible loop, the motion of which appears important for allowing early changes at D149. A serine-to-proline substitution could profoundly affect flexibility of this loop and thus modify the allosteric response to ligand binding. P320 interacts with a number of hydrophobic residues in the core pivot that have changing phi/psi angles along pathway 3. Again, mutating a proline in this region could have a significant structural consequence. Finally, residues in the core pivot region have been implicated in the conformational change of homologous proteins in the LacI/GalR family (*71*, *72*).

The single core pivot mutations described herein have long-range functional impact and highlight the exquisite sensitivity of protein properties to changing only one side chain in the sequence. These results emphasize the challenges inherent in predicting functional characteristics from similarities between related amino acid sequences. Further, this works illustrates the limitations of relying upon any single experimental technique. Integration of biochemical analysis with the results from static structures, dynamics simulations, and functional/phenotypic selection were essential to understanding the unexpected consequences of core pivot mutations.

ACKNOWLEDGMENT

We thank Corey Elam for generating pCRE, Simon Sims and colleagues at Genosys Inc. for providing oligonucleotides and sequencing services, Eric T. Lee and Deepa Varshnay for assistance with early screening efforts, Dr. Jay Kirchner for LacI polyclonal antibody, Drs. Graham Palmer and Daniel

Jancura for access to the instrument and assistance with the magnetic circular dichroism measurements, Jan O. Kemnade for experimental assistance, and Dr. Sarah Bondos and members of the Matthews laboratory for vibrant discussions and effective feedback.

REFERENCES

1. Matthews, K. S., and Nichols, J. C. (1998) *Prog. Nucleic Acid Res. Mol. Biol. 58*, 127−164.
2. Sams, C. F., Vyas, N. K., Quiocho, F. A., and Matthews, K. S. (1984) *Nature 310*, 429−430.
3. Hars, U., Horlacher, R., Boos, W., Welte, W., and Diederichs, K. (1998) *Protein Sci. 7*, 2511−2521.
4. Quiocho, F. A., and Ledvina, P. S. (1996) *Mol. Microbiol. 20*, 17−25.
5. Vyas, N. K., Vyas, M. N., and Quiocho, F. A. (1991) *J. Biol. Chem. 266*, 5226−5237.
6. Bell, C. E., and Lewis, M. (2000) *Nat. Struct. Biol. 7*, 209−214.
7. Lewis, M., Chang, G., Horton, N. C., Kercher, M. A., Pace, H. C., Schumacher, M. A., Brennan, R. G., and Lu, P. Z. (1996) *Science 271*, 1247−1254.
8. Schumacher, M. A., Choi, K. Y., Zalkin, H., and Brennan, R. G. (1994) *Science 266*, 763−770.
9. Schumacher, M. A., Choi, K. Y., Lu, F., Zalkin, H., and Brennan, R. G. (1995) *Cell 83*, 147−155.
10. Bessis, A. S., Bertrand, H. O., Galvez, T., De Colle, C., Pin, J. P., and Acher, F. (2000) *Protein Sci. 9*, 2200−2209.
11. Felder, C. B., Graul, R. C., Lee, A. Y., Merkle, H. P., and Sadee, W. (1999) *AAPS Pharm. Sci. 1*, E2.
12. Galvez, T., Parmentier, M. L., Joly, C., Malitschek, B., Kaupmann, K., Kuhn, R., Bittiger, H., Froestl, W., Bettler, B., and Pin, J. P. (1999) *J. Biol. Chem. 274*, 13362−13369.
13. Kunishima, N., Shimada, Y., Tsuji, Y., Sato, T., Yamamoto, M., Kumasaka, T., Nakanishi, S., Jingami, H., and Morikawa, K. (2000) *Nature 407*, 971−977.
14. Pin, J. P., Galvez, T., and Prezeau, L. (2003) *Pharmacol. Ther. 98*, 325−354.
15. Weickert, M. J., and Adhya, S. (1992) *J. Biol. Chem. 267*, 15869−15874.
16. Bessis, A. S., Rondard, P., Gaven, F., Brabet, I., Triballeau, N., Prezeau, L., Acher, F., and Pin, J. P. (2002) *Proc. Natl. Acad. Sci. U.S.A. 99*, 11097−11102.
17. Galvez, T., Duthey, B., Kniazeff, J., Blahos, J., Rovelli, G., Bettler, B., Prezeau, L., and Pin, J. P. (2001) *EMBO J. 20*, 2152−2159.
18. Galvez, T., and Pin, J. P. (2003) *Med. Sci. (Paris) 19*, 559−565.
19. Bell, C. E., and Lewis, M. (2001) *J. Mol. Biol. 312*, 921−926.
20. Friedman, A. M., Fischmann, T. O., and Steitz, T. A. (1995) *Science 268*, 1721−1727.
21. Schlitter, J., Engels, M., Kruger, P., Jacoby, E., and Wollmer, A. (1993) *Mol. Simul. 10*, 291−308.
22. Schlitter, J., Engels, M., and Kruger, P. (1994) *J. Mol. Graph. 12*, 84−89.
23. Flynn, T. C., Swint-Kruse, L., Kong, Y., Booth, C., Matthews, K. S., and Ma, J. (2003) *Protein Sci. 12*, 2523−2541.
24. Swint-Kruse, L., Elam, C. R., Lin, J. W., Wycuff, D. R., and Matthews, K. S. (2001) *Protein Sci. 10*, 262−276.
25. Falcon, C. M., and Matthew, K. S. (1999) *J. Biol. Chem. 274*, 30849−30857.
26. Fromant, M., Blanquet, S., and Plateau, P. (1998) in *Genetic Engineering with PCR* (Tait, R. C., Ed.) pp 39−55, Horizen Scientific Press, Norfolk, England.
27. Luria, S. E., Adams, J. N., and Ting, R. C. (1960) *Virology 12*, 348−390.
28. Swint-Kruse, L., Elam, C. R., Lin, J. W., Wycuff, D. R., and Matthews, K. S. (2001) *Protein Sci. 10*, 262−276.
29. Chakerian, A. E., and Matthews, K. S. (1991) *J. Biol. Chem. 266*, 22206−22214.
30. Murzin, A. G., Brenner, S. E., Hubbard, T., and Chothia, C. (1995) *J. Mol. Biol. 247*, 536−540.
31. Müller-Hill, B. (1983) *Nature 302*, 163−164.
32. von Wilcken-Bergmann, B., and Müller-Hill, B. (1982) *Proc. Natl. Acad. Sci. U.S.A. 79*, 2427−2431.
33. Meng, L. M., and Nygaard, P. (1990) *Mol. Microbiol. 4*, 2187−2192.
34. Horlacher, R., and Boos, W. (1997) *J. Biol. Chem. 272*, 13026−13032.
35. Rolfes, R. J., and Zalkin, H. (1990) *J. Bacteriol. 172*, 5637−5642.
36. Riggs, A. D., Newby, R. F., and Bourgeois, S. (1970) *J. Mol. Biol. 51*, 303−314.
37. Looger, L. L., Dwyer, M. A., Smith, J. J., and Hellinga, H. W. (2003) *Nature 423*, 185−190.
38. Miller, J. H. (1992) *A Short Course in Bacterial Genetics: A Laboratory Handbook for Escherichia coli and Related Bacteria*, Cold Spring Laboratory Press, Plainview, NY.
39. Vaara, M., and Vaara, T. (1983) *Antimicrob. Agents Chemother. 24*, 107−113.
40. Vaara, M. (1992) *Microbiol. Rev. 56*, 395−411.
41. Wycuff, D. R., and Matthews, K. S. (2000) *Anal. Biochem. 277*, 67−73.
42. Chen, J., and Matthews, K. S. (1992) *J. Biol. Chem. 267*, 13843−13850.
43. Falcon, C. M., Swint-Kruse, L., and Matthews, K. S. (1997) *J. Biol. Chem. 272*, 26818−26821.
44. O'Gorman, R. B., Dunaway, M., and Matthews, K. S. (1980) *J. Biol. Chem. 255*, 10100−10106.
45. Riggs, A. D., and Bourgeois, S. (1968) *J. Mol. Biol. 34*, 361−364.
46. Wong, I., and Lohman, T. M. (1993) *Proc. Natl. Acad. Sci. U.S.A. 90*, 5428−5432.
47. Holmquist, B., and Vallee, B. L. (1973) *Biochemistry 12*, 4409−4417.
48. Edelhoch, H. (1967) *Biochemistry 6*, 1948−1954.
49. Gardner, J. A., and Matthews, K. S. (1990) *J. Biol. Chem. 265*, 21061−21067.
50. Gilbert, W., and Maxam, A. (1973) *Proc. Natl. Acad. Sci. U.S.A. 70*, 3581−3584.
51. Johnson, M. L., and Faunt, L. M. (1992) *Methods Enzymol. 210*, 1−37.
52. Laiken, S. L., Gross, C. A., and von Hippel, P. H. (1972) *J. Mol. Biol. 66*, 143−155.
53. O'Gorman, R. B., Rosenberg, J. M., Kallai, O. B., Dickerson, R. E., Itakura, K., Riggs, A. D., and Matthews, K. S. (1980) *J. Biol. Chem. 255*, 10107−10114.
54. Daly, T. J., and Matthews, K. S. (1986) *Biochemistry 25*, 5474−5478.
55. Daly, T. J., and Matthews, K. S. (1986) *Biochemistry 25*, 5479−5484.
56. Chen, J., and Matthews, K. S. (1994) *Biochemistry 33*, 8728−8735.
57. Barry, J. K., and Matthews, K. S. (1999) *Biochemistry 38*, 6520−6528.
58. Suckow, J., Markiewicz, P., Kleina, L. G., Miller, J., Kisters-Woike, B., and Müller-Hill, B. (1996) *J. Mol. Biol. 261*, 509−523.
59. Pace, H. C., Kercher, M. A., Lu, P., Markiewicz, P., Miller, J. H., Chang, G., and Lewis, M. (1997) *Trends Biochem. Sci. 22*, 334−339.
60. Kleina, L. G., and Miller, J. H. (1990) *J. Mol. Biol. 212*, 295−318.
61. Markiewicz, P., Kleina, L. G., Cruz, C., Ehret, S., and Miller, J. H. (1994) *J. Mol. Biol. 240*, 421−433.
62. Chakerian, A. E., Tesmer, V. M., Manly, S. P., Brackett, J. K., Lynch, M. J., Hoh, J. T., and Matthews, K. S. (1991) *J. Biol. Chem. 266*, 1371−1374.
63. Falcon, C. M., and Matthews, K. S. (1999) *J. Biol. Chem. 274*, 30849−30857.
64. Jobe, A., and Bourgeois, S. (1972) *J. Mol. Biol. 69*, 397−408.
65. Barkley, M. D., Riggs, A. D., Jobe, A., and Bourgeois, S. (1975) *Biochemistry 14*, 1700−1712.
66. Chakerian, A. E., Olson, J. S., and Matthews, K. S. (1987) *Biochemistry 26*, 7250−7255.
67. Matthews, K. S., Falcon, C. M., and Swint-Kruse, L. (2000) *Nat. Struct. Biol. 7*, 184−187.
68. Barry, J. K., and Matthews, K. S. (1999) *Biochemistry 38*, 3579−3590.
69. Falcon, C. M., and Matthews, K. S. (2000) *Biochemistry 39*, 11074−11083.
70. Falcon, C. M., and Matthews, K. S. (2001) *Biochemistry 40*, 15650−15659.
71. Huffman, J. L., Lu, F., Zalkin, H., and Brennan, R. G. (2002) *Biochemistry 41*, 511−520.

72. Lu, F., Brennan, R. G., and Zalkin, H. (1998) *Biochemistry 37*, 15680−15690.
73. Sobolev, V., Sorokine, A., Prilusky, J., Abola, E. E., and Edelman, M. (1999) *Bioinformatics 15*, 327−332.
74. Swint-Kruse, L., Larson, C., Pettitt, B. M., and Matthews, K. S. (2002) *Protein Sci. 11*, 778−794.

BI035116X